

SAM Meets Robotic Surgery: An Empirical Study in Robustness Perspective

An Wang[†], Mobarakol Islam[†], Mengya Xu, Yang Zhang, Hongliang Ren^{*}

Abstract—Segment Anything Model (SAM) is a foundation model for semantic segmentation and shows excellent generalization capability with the prompts. In this empirical study, we investigate the robustness and zero-shot generalizability of the SAM in the domain of robotic surgery in various settings of (i) prompted vs. unprompted; (ii) bounding box vs. points-based prompt; (iii) generalization under corruptions and perturbations with five severity levels; and (iv) state-of-the-art supervised model vs. SAM. We conduct all the observations with two well-known robotic instrument segmentation datasets of MICCAI EndoVis 2017 and 2018 challenges. Our extensive evaluation results reveal that although SAM shows remarkable zero-shot generalization ability with bounding box prompts, it struggles to segment the whole instrument with point-based prompts and unprompted settings. Furthermore, our qualitative figures demonstrate that the model either failed to predict the parts of the instrument mask (e.g., jaws, wrist) or predicted parts of the instrument as different classes in the scenario of overlapping instruments within the same bounding box or with the point-based prompt. In fact, it is unable to identify instruments in some complex surgical scenarios of blood, reflection, blur, and shade. Additionally, SAM is insufficiently robust to maintain high performance when subjected to various forms of data corruption. Therefore, we can argue that SAM is not ready for downstream surgical tasks without further domain-specific fine-tuning.

Index Terms—Segment Anything, SAM, Robotic Surgery, Instrument Segmentation, Zero-shot Generalization, Robustness.

1 INTRODUCTION

SEGMENTATION of surgical instruments and tissue is a crucial challenge for robot-assisted surgery, and it is essential for instrument tracking and position estimation in surgical scenes. However, present deep learning models are frequently specialized to specific surgical sites, and their generalization capacity is restricted. As a result, establishing foundation models that can adapt to diverse surgical scenes and segmentation aims is critical in advancing robotic surgery [1]. Recently, segmentation foundation models have made great progress in the field of natural image segmentation. The segment anything model (SAM) [2], which has been trained on more than 1 billion masks and has significant skills for creating accurate object masks based on prompts (e.g., bounding boxes, points, sentences), is the original and best-known segmentation foundation model. Several works have revealed that SAM can fail on common medical image segmentation tasks [3], [4], [5], [6]. This is reasonable and predictable given that SAM’s training set consists primarily of natural image datasets with substantial edge information. Evaluating the performance of SAM on surgical scenes remains an underexplored field with scope to investigate further. In this report, we evaluate the generalizability of SAM under bounding box and point prompted settings on two public robotic surgery datasets.

2 EXPERIMENTS

In this study, two widely-used surgical instrument segmentation datasets, *i.e.*, EndoVis17 [7] and EndoVis18 [8], have been adopted in our experiments. Our evaluation involves three categories. Firstly, we have provided both quantitative and qualitative assessments on the promptable segmentation performance of SAM, with bounding boxes and single points, for binary and instrument-wise segmentation. Besides, we comprehensively test the robustness of SAM with 18 types of data corruption at 5 severity levels by following [9]. Moreover, we also examine SAM on its automatic mask generation in unprompted settings for surgical scene segmentation.

2.1 Experimental Settings

Datasets. We have employed two classical datasets in endoscopic surgical instrument segmentation, *i.e.*, EndoVis17 [7] and EndoVis18 [8]. We follow the data splits in previous works [10], [11], [12] to conduct the evaluation for SAM.

Prompts. The original EndoVis datasets [7], [8] do not have bounding boxes or point annotations. We have labeled the datasets with bounding boxes for each instrument, associated with corresponding class information. Additionally, regarding the single-point prompt, we obtain the center of each instrument mask by simply computing the moments of the mask contour. Since SAM [2] only predicts binary segmentation masks, for instrument-wise segmentation, the output instrument labels are assigned inherited from the input prompts.

Metrics. The IoU and Dice metrics from the EndoVis17 [7] challenge¹ is used. Specifically, only the classes presented in a frame are considered in the calculation for instrument segmentation.

- An Wang, Yang Zhang, and Hongliang Ren are with the Department of Electronic Engineering, The Chinese University of Hong Kong, Hong Kong SAR, China.
- Mobarakol Islam is with the Wellcome/EPSRC Centre for Interventional and Surgical Sciences (WEISS), Department of Medical Physics and Biomedical Engineering, University College London, UK.
- Mengya Xu and Hongliang Ren are with the Department of Biomedical Engineering, National University of Singapore, Singapore.
- Yang Zhang is with the School of Mechanical Engineering, Hubei University of Technology, China.
- Corresponding author: Hongliang Ren (hlren@ee.cuhk.edu.hk).
- An Wang and Mobarakol Islam are co-first author.

1. <https://github.com/ternaus/robot-surgery-segmentation>

TABLE 1

Quantitative comparison of different methods for binary and instrument segmentation on EndoVis17 [7] and EndoVis18 [8] datasets. The adopted metric is the IoU (%) in EndoVis17 Challenge [7]. The best and runner-up results are shown in bold and underlined, respectively. With bounding boxes as prompts, SAM [2] shows superior performance compared with other methods. BBOX denotes for bounding box.

Type	Method	Pub/Year(20-)	Arch.	EndoVis17 [7]		EndoVis18 [8]	
				Binary IoU	Instrument IoU	Binary IoU	Instrument IoU
Single-Task	Vanilla UNet [13]	MICCAI15	UNet [13]	75.44	15.80	<u>68.89</u>	-
	TernausNet [10]	ICMLA18	UNet [13]	83.60	35.27	-	46.22
	MF-TAPNet [12]	MICCAI19	UNet [13]	87.56	37.35	-	67.87
	Islam <i>et al.</i> [14]	RA-L19	-	84.50	-	-	-
	ISINet [11]	MICCAI21	Res50 [21]	-	55.62	-	73.03
	Wang <i>et al.</i> [15]	MICCAI22	UNet [13]	-	-	58.12	-
Multi-Task	ST-MTL [16]	MedIA21	-	83.49	-	-	-
	AP-MTL [18]	ICRA20	-	<u>88.75</u>	-	-	-
	S-MTL [17]	RA-L22	-	-	-	-	43.54
	TraSeTR [19]	ICRA22	Res50 [21] + Trfm [22]	-	60.40	-	<u>76.20</u>
	S3Net [20]	WACV23	Res50 [21]	-	<u>72.54</u>	-	<u>75.81</u>
Prompt-based	SAM [2] 1 Point	arxiv23	ViT [23]	53.88	55.96	57.12	54.30
	SAM [2] BBox	arxiv23	ViT [23]	89.19	88.20	89.35	81.09

TABLE 2

Quantitative results on different splits of EndoVis17 [7] and EndoVis18 [8] datasets.

Method	EndoVis17 [7] (Seq9, Seq10)				EndoVis18 [8] (Train + Val)			
	Binary		Instrument		Binary		Instrument	
	IoU	Dice	IoU	Dice	IoU	Dice	IoU	Dice
SAM 1 Point	58.99	71.04	57.19	67.68	59.81	70.89	57.43	65.91
SAM BBox	90.41	94.86	86.58	91.32	87.15	92.64	81.08	86.53

TABLE 3

Quantitative results on synthetic EndoVis18 [8] validation data with various corruptions. 18 types of corruptions from 4 categories are employed to construct the synthetic datasets. Each corruption has 5 severity levels, and level 0 indicates clean data. The adopted metric is the IoU (%) from EndoVis17 Challenge [7]. SAM [2] encounters severe performance degradation in most cases but reacts differently to various types and levels of data corruption.

Severity	Noise				Blur				Weather				Digital						
	Gaussian	Shot	Impulse	Speckle	Defocus	Glass	Motion	Zoom	Gaussian	Snow	Frost	Fog	Bright	Spatter	Contrast	Pixel	JPEG	Saturate	
0	89.35																		
Binary	1	77.69	80.18	80.43	83.28	82.01	80.53	82.99	80.30	85.40	84.08	83.12	85.38	87.43	86.69	85.76	81.12	58.77	86.64
	2	73.92	76.07	76.15	81.65	80.21	79.20	80.22	77.55	81.69	80.69	80.34	84.65	87.27	84.21	84.90	79.32	56.04	84.85
	3	69.21	71.74	73.02	77.74	76.96	72.64	75.50	75.27	78.31	79.58	78.90	83.62	87.23	82.50	83.36	73.81	56.25	86.84
	4	63.80	65.41	67.29	75.28	73.79	72.38	69.60	73.22	75.23	76.33	78.38	82.28	87.06	83.12	77.12	70.82	57.59	83.21
	5	57.07	60.61	61.61	71.83	69.85	69.59	66.25	71.58	66.96	77.66	76.82	78.84	86.43	79.62	66.58	68.55	56.77	81.26
Instrument	0	81.09																	
	1	69.51	71.83	72.25	74.82	73.64	72.13	74.33	71.41	76.79	75.40	74.42	76.82	79.16	78.24	77.17	72.94	54.86	78.27
	2	66.06	68.09	68.53	73.19	71.74	71.02	71.46	68.85	73.15	72.13	71.65	76.14	79.00	75.54	76.22	71.55	52.23	76.61
	3	62.01	64.44	65.89	69.75	68.74	64.97	67.13	67.12	70.08	70.97	70.21	75.01	78.90	73.70	74.67	66.83	51.63	78.39
	4	57.28	59.12	61.03	67.82	65.87	64.87	62.15	65.18	67.23	68.43	69.79	73.73	78.73	74.24	69.48	63.99	51.88	74.91
	5	51.56	55.16	55.86	64.76	62.43	62.23	59.26	63.96	60.60	69.33	68.32	70.45	78.19	70.72	61.14	61.79	51.01	73.35

Comparison methods. We have involved several classical and recent methods, including the vanilla UNet [13], TernausNet [10], MF-TAPNet [12], Islam *et al.* [14], Wang *et al.* [15], ST-MTL [16], S-MTL [17], AP-MTL [18], ISINet [11], TraSeTR [19], and S3Net [20] for surgical binary and instrument-wise segmentation. The ViT-H-based SAM [2] is employed in all our investigations. Note that we cannot provide an absolutely fair comparison because existing methods do not need prompts during inference.

2.2 Surgical Instruments Segmentation with Prompts

2.2.1 Implementation

With bounding boxes and single points as prompts, we input the images to SAM [2] to get the predicted binary masks for the target

objects. Because SAM [2] can not provide consistent categorical information. We compromise to use the class information from the bounding boxes directly. In this way, we derive instrument-wise segmentation while bypassing the possible errors from misclassifications, an essential factor affecting instrument-wise segmentation accuracy.

2.2.2 Results and Analysis

SAM [2], as a foundational segmentation model, also exhibits great generalization capability in robotic surgery scenes. As shown in Table 1, with bounding boxes as prompts, SAM [2] outperforms previous unprompted supervised methods in binary and instrument-wise segmentation on both datasets. Besides, when tested on different data splits settings, as presented in Table 2,

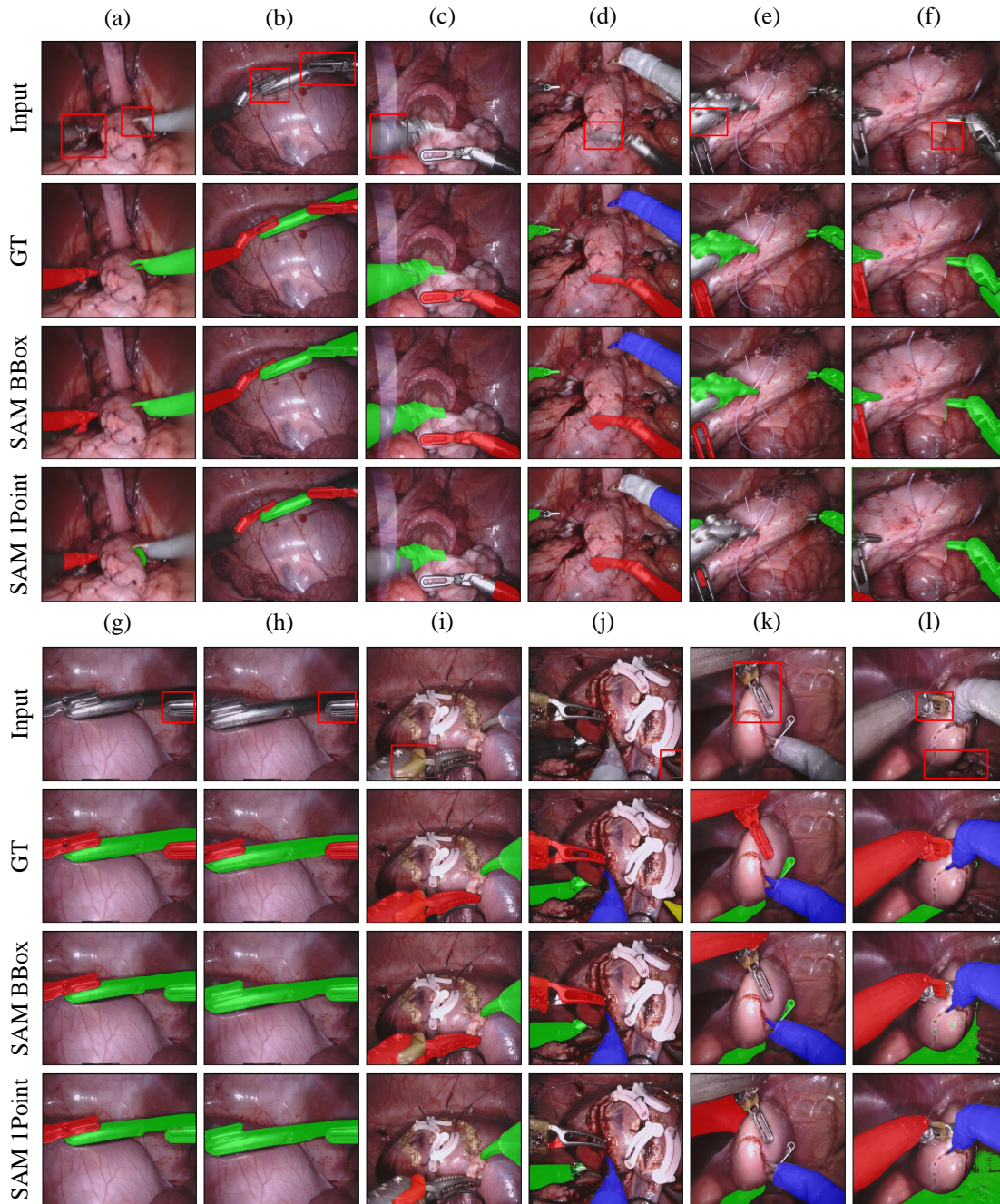


Fig. 1. **Qualitative results of SAM [2] on some challenging frames.** Red rectangles highlight the typical challenging regions which cause unsatisfactory predictions. Detailed analyses of each case are provided in the Result section.

SAM [2] still maintains its performance. These results demonstrate its superiority in generalizing to unseen endoscopic data under bounding box prompt of the surgical domains. With single points as prompts, SAM [2] degrades a lot in performance, indicating its limited ability to segment surgical instruments from weak prompts. This reveals the performance of the SAM is closely rely on the heavy prompts.

For complicated surgical scenes, SAM [2] still struggles to produce accurate segmentation results, as shown in columns (a) to (l) of Fig. 1. Typical challenges, including shadows (a), motion blur (d), occlusion (b, g, h), light reflection (c), insufficient light (j, l), over brightness (e), ambiguous suturing thread (f), instrument

wrist (i), and irregular instrument pose (k), all lead to unsatisfied segmentation performance.

2.3 Robustness under Data Corruption

2.3.1 Implementation

Referring to the robustness evaluation benchmark [9], we have evaluated SAM [2] under 18 types of data corruptions at 5 severity levels with the official implementations². Note that the *Elastic Transformation* has been omitted to avoid inconsistency between the input image and associated masks. The adopted data corruption

2. <https://github.com/hendrycks/robustness>

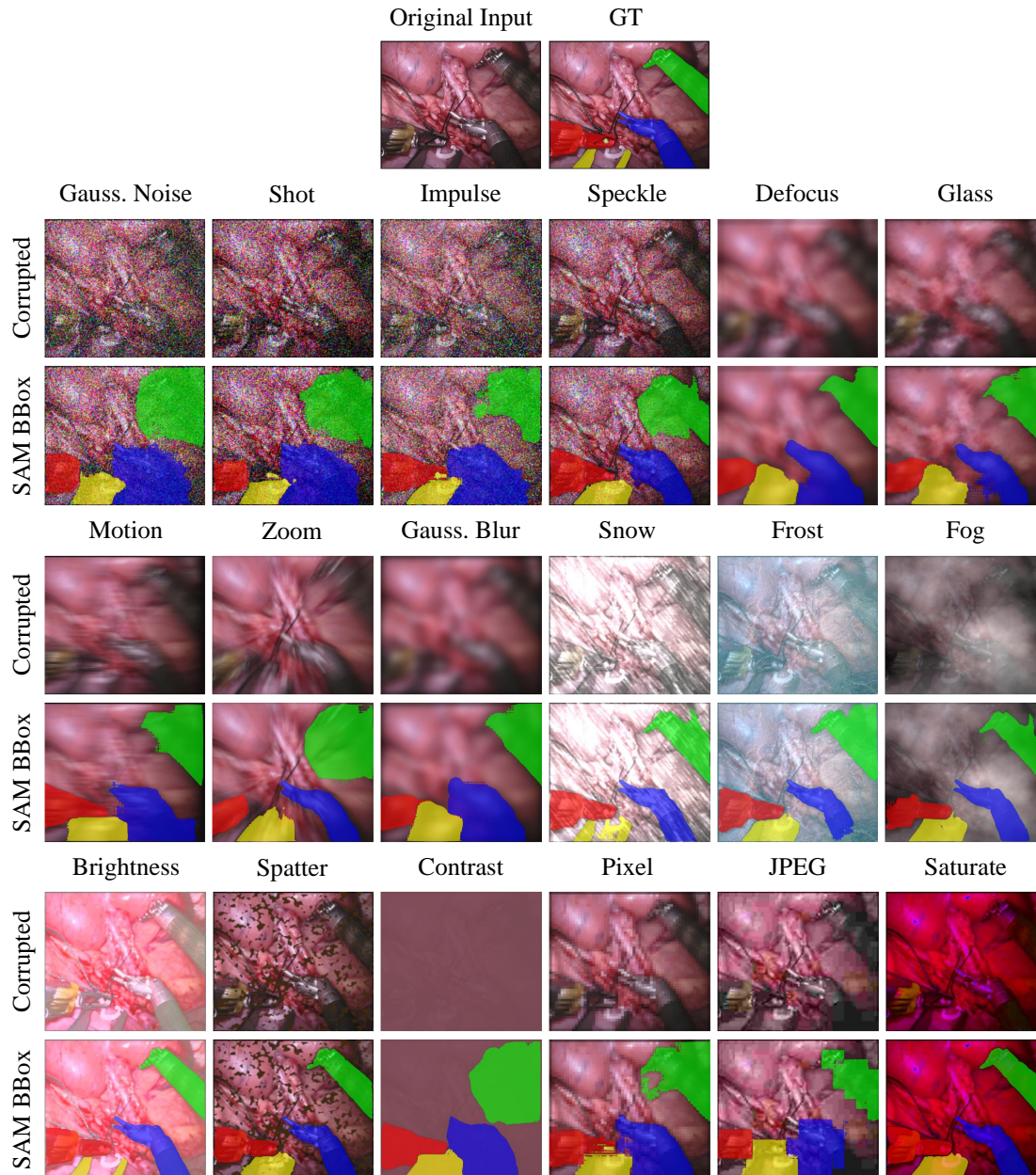


Fig. 2. **Qualitative results of SAM [2] under 18 data corruptions of level-5 severity.** Bounding boxes are adopted as the prompts. SAM [2] can hardly maintain segmentation performance for most types of data corruption, showing its limited capacity for robustness.

can be allocated into four distinct categories of *Noise*, *Blue*, *Weather*, and *Digital*.

2.3.2 Results and Analysis

The severity of data corruption is directly proportional to the degree of performance degradation in SAM [2], as depicted in Table 3. The resilience of the SAM algorithm [2] may be influenced differently depending on the nature of the corruption present. However, in the majority of scenarios, the algorithm’s performance diminishes significantly. Among the various types of corruption, *JPEG Compression* and *Gaussian Noise* have the greatest impact on segmentation performance, whereas *Brightness* has a negligible effect. Figure 2 presents one exemplar frame in its original state, alongside various corrupted versions at a severity level of 5). We can observe that SAM [2] still suffers great performance degradation in most cases.

2.4 Automatic Surgical Scene Segmentation

2.4.1 Implementation

Without prompts, SAM [2] also supports automatic mask generation in unprompted setting. For naive investigation of the automatic surgical scene segmentation results, we use the default parameters from the official implementation³ without further tuning. The colors of each segmented mask are randomly assigned because SAM [2] only generates binary masks for each object.

2.4.2 Results and Analysis

As shown in Fig. 3, in surgical scene segmentation, SAM [2] can produce promising results on simple scenes like columns (a) and (f). But it encounters difficulties when applied to more

3. <https://github.com/facebookresearch/segment-anything>

complicated scenes, as it struggles to differentiate between the entirety of instrument articulating parts accurately and to identify discrete tissue structures as interconnected units. As a foundation model, SAM [2] still lacks comprehensive awareness of objects' semantics, especially in downstream domains like surgical scenes.

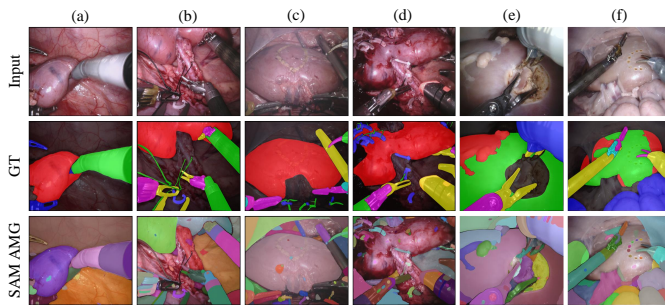


Fig. 3. **Automatic mask generation (AMG) in unprompted setting from SAM [2] for EndoVis18 [8] scene segmentation.** SAM [2] cannot provide consistent categorical labels for each mask, and its comprehension of the proper surgical scene semantics is limited, leading to disconnected instrument articulating parts and fragmented anatomical tissue structures.

3 CONCLUSION

In this study, we explore the robustness and zero-shot generalizability of the SAM [2] in the field of robotic surgery on two robotic instrument segmentation datasets of MICCAI EndoVis 2017 and 2018 challenges, respectively. Extensive empirical results suggest that SAM [2] is deficient in segmenting the entire instrument with point-based prompts and unprompted settings, as clearly shown in Fig. 1 and Fig. 3. This implies that SAM [2], although yielding surprising zero-shot generalization ability, can still not capture the surgical scenes precisely. Besides, it exhibits challenges in accurately predicting certain parts of the instrument mask when there are overlapping instruments or only with a point-based prompt. It also fails to identify instruments in complex surgical scenarios, such as blood, reflection, blur, and shade. Last but not least, we extensively evaluate the robustness of SAM [2] with a wide range of data corruptions. As indicated by Table 3 and Fig. 2, SAM [2] encounters significant performance degradation in many scenarios.

As a foundational segmentation model, SAM [2] shows remarkable generalization capability in robotic surgical segmentation, yet it still suffers performance degradation due to downstream domain shift, data corruptions, perturbations, and complex scenes. To further improve its performance, a broad spectrum of evaluations and extensions, including fine-tuning, should be explored and developed.

REFERENCES

- [1] L. Seenivasan, M. Islam, G. Kannan, and H. Ren, "Surgicalgpt: End-to-end language-vision gpt for visual question answering in surgery," *arXiv preprint arXiv:2304.09974*, 2023.
- [2] A. Kirillov, E. Mintun, N. Ravi, H. Mao, C. Rolland, L. Gustafson, T. Xiao, S. Whitehead, A. C. Berg, W.-Y. Lo *et al.*, "Segment anything," *arXiv preprint arXiv:2304.02643*, 2023.
- [3] R. Deng, C. Cui, Q. Liu, T. Yao, L. W. Remedios, S. Bao, B. A. Landman, L. E. Wheless, L. A. Coburn, K. T. Wilson *et al.*, "Segment anything model (sam) for digital pathology: Assess zero-shot segmentation on whole slide imaging," *arXiv preprint arXiv:2304.04155*, 2023.
- [4] C. Hu and X. Li, "When sam meets medical images: An investigation of segment anything model (sam) on multi-phase liver tumor segmentation," *arXiv preprint arXiv:2304.08506*, 2023.
- [5] S. He, R. Bao, J. Li, P. E. Grant, and Y. Ou, "Accuracy of segment-anything model (sam) in medical image segmentation tasks," *arXiv preprint arXiv:2304.09324*, 2023.
- [6] J. Ma and B. Wang, "Segment anything in medical images," 2023.
- [7] M. Allan, A. Shvets, T. Kurmann, Z. Zhang, R. Duggal, Y.-H. Su, N. Rieke, I. Laina, N. Kalavakonda, S. Bodenstedt *et al.*, "2017 robotic instrument segmentation challenge," *arXiv preprint arXiv:1902.06426*, 2019.
- [8] M. Allan, S. Kondo, S. Bodenstedt, S. Leger, R. Kadkhodamohammadi, I. Luengo, F. Fuentes, E. Flouty, A. Mohammed, M. Pedersen *et al.*, "2018 robotic scene segmentation challenge," *arXiv preprint arXiv:2001.11190*, 2020.
- [9] D. Hendrycks and T. Dietterich, "Benchmarking neural network robustness to common corruptions and perturbations," in *International Conference on Learning Representations*, 2019.
- [10] A. A. Shvets, A. Rakhlin, A. A. Kalinin, and V. I. Iglovikov, "Automatic instrument segmentation in robot-assisted surgery using deep learning," in *2018 17th IEEE International Conference on Machine Learning and Applications (ICMLA)*, 2018, pp. 624–628.
- [11] C. González, L. Bravo-Sánchez, and P. Arbelaez, "Isinet: an instance-based approach for surgical instrument segmentation," in *Medical Image Computing and Computer Assisted Intervention—MICCAI 2020: 23rd International Conference, Lima, Peru, October 4–8, 2020, Proceedings, Part III 23*. Springer, 2020, pp. 595–605.
- [12] Y. Jin, K. Cheng, Q. Dou, and P.-A. Heng, "Incorporating temporal prior from motion flow for instrument segmentation in minimally invasive surgery video," in *Medical Image Computing and Computer Assisted Intervention—MICCAI 2019: 22nd International Conference, Shenzhen, China, October 13–17, 2019, Proceedings, Part V 22*. Springer, 2019, pp. 440–448.
- [13] O. Ronneberger, P. Fischer, and T. Brox, "U-net: Convolutional networks for biomedical image segmentation," in *Medical Image Computing and Computer-Assisted Intervention—MICCAI 2015: 18th International Conference, Munich, Germany, October 5–9, 2015, Proceedings, Part III 18*. Springer, 2015, pp. 234–241.
- [14] M. Islam, D. A. Atputharuban, R. Ramesh, and H. Ren, "Real-time instrument segmentation in robotic surgery using auxiliary supervised deep adversarial learning," *IEEE Robotics and Automation Letters*, vol. 4, no. 2, pp. 2188–2195, 2019.
- [15] A. Wang, M. Islam, M. Xu, and H. Ren, "Rethinking surgical instrument segmentation: A background image can be all you need," in *International Conference on Medical Image Computing and Computer-Assisted Intervention*. Springer, 2022, pp. 355–364.
- [16] M. Islam, V. Vibashan, C. M. Lim, and H. Ren, "St-mtl: Spatio-temporal multitask learning model to predict scanpath while tracking instruments in robotic surgery," *Medical Image Analysis*, vol. 67, p. 101837, 2021.
- [17] L. Seenivasan, S. Mitheran, M. Islam, and H. Ren, "Global-reasoned multi-task learning model for surgical scene understanding," *IEEE Robotics and Automation Letters*, vol. 7, no. 2, pp. 3858–3865, 2022.
- [18] M. Islam, V. Vibashan, and H. Ren, "Ap-mtl: Attention pruned multi-task learning model for real-time instrument detection and segmentation in robot-assisted surgery," in *2020 IEEE international conference on robotics and automation (ICRA)*. IEEE, 2020, pp. 8433–8439.
- [19] Z. Zhao, Y. Jin, and P.-A. Heng, "Trasetr: track-to-segment transformer with contrastive query for instance-level instrument segmentation in robotic surgery," in *2022 International Conference on Robotics and Automation (ICRA)*. IEEE, 2022, pp. 11 186–11 193.
- [20] B. Baby, D. Thapar, M. Chasmai, T. Banerjee, K. Dargan, A. Suri, S. Banerjee, and C. Arora, "From forks to forceps: A new framework for instance segmentation of surgical instruments," in *Proceedings of the IEEE/CVF Winter Conference on Applications of Computer Vision*, 2023, pp. 6191–6201.
- [21] K. He, X. Zhang, S. Ren, and J. Sun, "Deep residual learning for image recognition. arxiv 2015," *arXiv preprint arXiv:1512.03385*, vol. 14, 2015.
- [22] A. Vaswani, N. Shazeer, N. Parmar, J. Uszkoreit, L. Jones, A. N. Gomez, Ł. Kaiser, and I. Polosukhin, "Attention is all you need," *Advances in neural information processing systems*, vol. 30, 2017.
- [23] A. Dosovitskiy, L. Beyer, A. Kolesnikov, D. Weissenborn, X. Zhai, T. Unterthiner, M. Dehghani, M. Minderer, G. Heigold, S. Gelly, J. Uszkoreit, and N. Houlsby, "An image is worth 16x16 words: Transformers for image recognition at scale," in *International Conference on Learning Representations*, 2021.